Journal of Chromatographic Science 2015;53:1092–1099
doi:10.1093/chromsci/bmu171 Advance Access publication December 29, 2014

Article

Metabolism Study of Veratramine Associated with Neurotoxicity by Using HPLC–MS^n

Yue Cong[1,2], Jinggong Guo[3], Zhi Tang[2], Shuhai Lin[2], Qingchun Zhang[1], Jing Li[1] and Zongwei Cai[2]*

[1]Institute of Pharmacy, Pharmaceutical College, Henan University, Kaifeng, China, [2]Department of Chemistry, Hong Kong Baptist University, Kowloon, Hong Kong, and [3]The Key Laboratory of Plant Stress Biology, Henan University, Kaifeng, China

*Author to whom correspondence should be addressed. Email: zwcai@hkbu.edu.hk

Received 13 January 2014; revised 8 September 2014

Veratramine (VAM) is the major lipid-soluble alkaloid existing in *Veratrum nigrum* L. that has been demonstrated to exert neurotoxic effects. To better understand the potential mechanism of neurotoxicity of VAM, VAM-induced DNA damage was measured in the cerebellum and cerebral cortex of mice after a 7-day repetitive oral dose by using single-cell gel electrophoresis (comet assay). A method based on high-performance liquid chromatography–electrospray ionization tandem mass spectrometry was developed for the determination of VAM and its *in vivo* and *in vitro* metabolites, to establish the potential correlation between metabolites and neurotoxicity. *In vitro* experiment was carried out using rat liver microsomes, whereas the *in vivo* study was conducted on rats at a single dose of 3 mg/kg. The results showed that VAM caused DNA damage in the cerebellum and cerebral cortex of mice in a dose-dependent manner. Phenyl mono-oxidation, sulfate conjugation and phenyl di-oxidation were proposed to be the main *in vivo* metabolic pathways of VAM, whereas the major *in vitro* metabolic pathways were phenyl mono-oxidation, hydroxylation and methylation. Phenyl-oxidation reaction was likely to be associated with reactive oxygen species production, leading to the DNA damage in the mouse brain.

Introduction

Veratrum nigrum L., a traditional Chinese medicine (TCM), was originally used for the treatment of hypertension, apoplexy, excessive phlegm, etc. (1). However, the clinical use of *V. nigrum* L. was declined due to the high risk of neurotoxicity (2–4). *Veratrum* alkaloids were proved to be the major bioactive and toxic ingredients with genotoxicity (3, 5, 6), reproductive toxicity (7) and neurotoxicity (3, 8). As a major *Veratrum* alkaloid (9), veratramine (VAM) (Figure 1) is significantly effective against hypertension by reflective inhibition of vasomotor center (10) and tumor as an antagonist of the hedgehog signaling (11, 12). Furthermore, VAM can reduce the rate of spontaneous depolarization of sinoatrial node cells throughout diastole (13). However, it was regrettable to discover that VAM could induce teratogenic effects (14) and 5-HT syndrome as a releaser and uptake inhibitor of 5-HT (15). The lethal dose 50% (LD_{50}) of VAM for mice is 15.9 mg/kg with intragastrical administration (10).

In our previous study, it was proved that *Veratrum* alkaloids could cause DNA damage in the cerebellum and cerebral cortex of mice by oxidative stress (3, 6). Recent studies have suggested that some toxic chemicals could be transformed by Phase I enzymes into DNA-reactive metabolites (16–18). For example, *in vitro* metabolites of veratridine, a natural neurotoxic steroidal alkaloid, in male rat liver microsomes were presumed to mediate the neurotoxicity via protein binging due to the formation of catechol structures (19). Inspired by this, we suspected that the bioactive component VAM and/or its metabolites might have the neurotoxic effect.

High-performance liquid chromatography coupled with electrospray ionization tandem mass spectrometry (HPLC–ESI-MS^n) is a more powerful technology for the analysis of metabolites of TCM. This approach is accurate, specific and sensitive for the analysis of metabolites of natural products in complex biological samples. By comparing changes of metabolites in retention times, molecular masses and fragmentation patterns with those of the parent drug, the metabolites can be identified.

Here, we perform the alkaline comet assay that has been widely used in both the *in vivo* and *in vitro* study to detect DNA damage and to delineate the genotoxic effect of VAM on brain cells in mice. The *in vivo* and *in vitro* metabolites of VAM were separated and identified using HPLC–ESI-MS^n. Data-dependent scanning in a positive mode was performed to obtain ESI-MS^3 data to characterize the structures of metabolites *in vivo* and *in vitro*. And, the metabolic transformation was also proposed to seek the potential relationship between metabolites and neurotoxicity of VAM, which may be helpful to understand the mechanism of the neurotoxic action of VAM.

Experimental

Materials and reagents

VAM (≥98%) was separated and purified according to procedures reported previously (20). NADPH and uridine diphosphate glucuronic acid (UDPGA) were purchased from Oriental Yeast Co., Ltd (Tokyo, Japan). Water was prepared using an Milli-Q reagent water system (Millipore, Billerica, MA, USA). HPLC grade methanol, acetonitrile and formic acid were purchased from Tedia (Fairfield, CT, USA). Potassium dihydrogen phosphate in ultra-pure grade was obtained from Mallinckrodt (Paris, KY, USA). Dimethyl sulfoxide (DMSO) in the analytical pure grade was purchased from AJAX Chemicals (Sydney, Australia). Dimethyl sulfate (DMS) in the analytical pure grade was obtained from Tianjin Fuchen Chemical Agencies (Tianjin, China). Other reagents used here were of analytical grade.

Instrumentation

HPLC–MS^n was performed on a Bruker Esquire-4000 ion-trap mass spectrometer (Bruker-Fransen, Bremen, Germany) equipped with electrospray ionization source couple to an Agilent 1100 HPLC system (Agilent Technologies, Palo Alto, CA, USA). A TurboVap LV evaporator was also used (Caliper Life Sciences, Hopkinton, MA, USA).

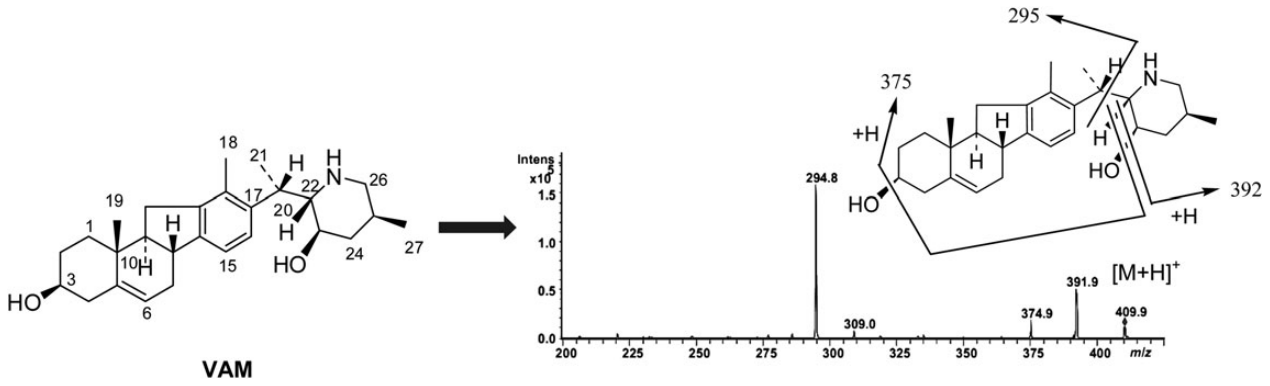

Figure 1. The structure and LC–ESI-MS spectrum of VAM.

Analytical conditions

Chromatographic separations were accomplished by using a Waters Symmetry C18 column (150 × 2.1 mm, 3.5 μm; Waters, Milford, MA, USA). The injection volume and column temperature were 5 μL and 22°C, respectively. The mobile phase consisted of 0.1% formic acid in water (Solvent A) and acetonitrile (Solvent B) and was delivered at a flow rate of 0.15 mL/min. The linear gradient elution program was used as follows: 15–50% B over 15 min and 50–100% B over 5 min. The composition was then held at 100% B for 5 min, and returned to initial conditions and equilibrated for 14.5 min. During the LC–MS^n analysis, up to 1.5 min of the initial flow was diverted to waste. A full-scan ESI-MS analysis at positive ion mode with a range of m/z 200–700 for VAM was performed. For MS^2 analysis, ion at m/z 410 for VAM and protonated ions of detected metabolites were selected with conditions of compound stability 60%, trap drive level 100%, collision energy 1 V, dry temperature 340°C, dry gas 9 L/min and nebulizer gas 35 psi. These chromatographic and mass spectrometric conditions were optimized for the use of VAM.

Animals

Male Swiss mice (22 ± 2 g) were obtained from the Experimental Animal Center of Zhengzhou University (Zhengzhou, China). Male Sprague–Dawley rats (~8 weeks old and average weight of 220 g) were purchased from the Laboratory Animal Service Center of the Chinese University of Hong Kong (Hong Kong, China). The animals were housed under standard conditions (22 ± 2°C temperature, 50 ± 10% relative humidity and 12L : 12D light–dark cycles). Food and water were available *ad libitum*. An acclimation period of at least 1 week was allowed for mice and rats prior to the drug administration.

All animal experiments were conducted according to the guidelines established by the NIH Guide for the Care and Use of Laboratory Animals. The protocols were approved by internal animal care and use committees of Hong Kong Baptist University (Hong Kong, China) and Henan University (Kaifeng, China).

Preparation of comet assay

Mice were randomly divided into four groups of four mice in each group, which included control, positive, VAM 0.25 μmol/kg and VAM 2.5 μmol/kg groups. The animals in the VAM groups were treated by gavage with VAM at 0.25 and 2.50 μmol/kg every day for consecutive 7 days. The control group was treated with distilled water for 7 days. At the last day, the positive group received an i.p. injection of DMS at 20 mg/kg. The comet assay was performed according to the previous reports (3, 6, 21). Tail moment was used as parameter to evaluate the DNA damage. Data were expressed as mean ± SEM calculated from four mice of every group. Statistical comparisons were made by means of one-way analysis of variance (ANOVA), followed by the Fisher's least significant difference (LSD) test (SPSS 17.0 software, SPSS, USA).

Preparation of rat liver microsomes

Rat liver microsomes were prepared as described previously (18). The pooled liver microsomal extracts were suspended in 0.1 M PBS (pH 7.4) and stored at −80°C before use. The rat liver microsomal CYP and protein concentrations were determined by the methods reported by Omura and Sato (22) and Bradford (23).

In vitro incubation conditions

The microsomal incubation conditions were established and controlled to provide a reproducible rate of the metabolism *in vitro*. A typical reaction mixture contained 100 mmol/L of PBS buffer (pH 7.4), 5 mmol/L of $MgCl_2$, 1 g/L of microsomal protein and 0.2 g/L of VAM in the final volume of 0.2 mL. The incubation mixture was preincubated at 37°C for 5 min and the reaction was initiated by adding NADPH (final concentration of 1.0 mmol/L), then incubated at 37°C in a water bath shaker for 60 min. The reaction was terminated by adding 0.8 mL of ice-cold acetonitrile, vortex-mixed for 10 s and centrifuged at 12,000 rpm for 15 min. The supernatant was transferred to a clean tube and evaporated under a gentle stream of nitrogen gas. Control incubations were carried out in the same manner, except that NADPH or parent drug was excluded. The incubation conditions of Phase II metabolism were the same as those of Phase I metabolism, except that UDPGA was used to replace NADPH.

Sample preparation of rat plasma, urine and feces

Rats separated into two groups ($n = 3$) were fasted 12 h prior to administration of the dose and fed 12 h after the dose, which was formulated in a mixture of sample suspended in 1% carboxy

methyl cellulose sodium salt (CMC-Na) solution at a target concentration of 0.4 mg/mL. They received sample solution by gavage administration with a single dosage of 3 mg/kg body weight.

Because elimination of *Veratrum* alkaloids in rats was quick (24, 25), blood samples were collected in heparinized tubes via caudal vein predose and at 0.5, 1, 2, 3, 4 and 5 h postdose. The plasma samples collected at 2.5 h postdose were selected for metabolite identification, owing to the highest peak abundance of VAM. Blank plasma was harvested from predose blood sample. For sample preparation, rat plasma (300 μL) was diluted with three volumes of acetonitrile and then centrifuged at 11,000 rpm for 10 min. The supernatant was pooled and blown to dry by using a gentle stream of N_2 at 35°C, then dissolved in 20 μL of acetonitrile and transferred to a clean tube for LC–MS^n analysis.

Another group of rats ($n = 3$) was housed individually in metabolic cages and dosed for the identification of excretory metabolites. Urine and feces predose samples, i.e. blanks, were collected at the end of interval of 0–24 h after a 12-h fasting period. Urine and feces postdose samples were collected into a clean container for 24 h interval postdose and stored frozen at −80°C until analysis.

Urine samples (5 mL) were diluted with three volumes of acetonitrile and centrifuged at 8,000 rpm for 10 min, and the supernatant was pooled and blown to dry by N_2 at 35°C. The residue was dissolved in acetonitrile and centrifuged at 11,000 rpm for 10 min. The supernatant was pooled and transferred to a clean tube for LC–MS^n analysis. Feces samples (10 g) were added to acetonitrile (3 mL/g feces) and mixed to generate the fecal homogenates, and then let stand for 4 h at room temperature. Feces samples were extracted two times. After filtration, the filtrates were evaporated to dryness at 35°C by using N_2. The residue was dissolved in acetonitrile and then centrifuged at 11,000 rpm for 10 min. The supernatant was pooled and transferred to a clean tube for LC–MS^n analysis.

Results

Effect of VAM administration on brain cells

After the oral administration of VAM at the doses of 0.25 and 2.50 μmol/kg every day for 7 consecutive days, comet assay was performed in the cells obtained from the cerebellum and cerebral cortex region in mice. The extent of DNA damage was calculated from relative changes in tail moment length. The obtained results showed that VAM significantly increased the values of tail moment length when compared with the control group (one-way ANOVA; $P < 0.001$; Figure 2), suggesting that VAM induced DNA damage in the mouse cerebellum and cerebral cortex following a 7-day repetitive dose. In addition, a dose-dependent increase in DNA damage indicated that this damage is chemical related. These two brain regions could be targeted for neurotoxicity of VAM and/or its metabolites. It is generally considered that DNA damage caused by chemicals increases the possibility of mutation and cancer (26).

Characteristics of rat liver microsomes

The rat liver microsomal CYP and protein concentrations were, respectively, 0.117 nmol/mg and 25.00 mg/mL within the normal range for *in vitro* metabolism. The difference was small between individual rats. These results suggested that the obtained microsomal samples could be used in the *in vitro* metabolism experiments.

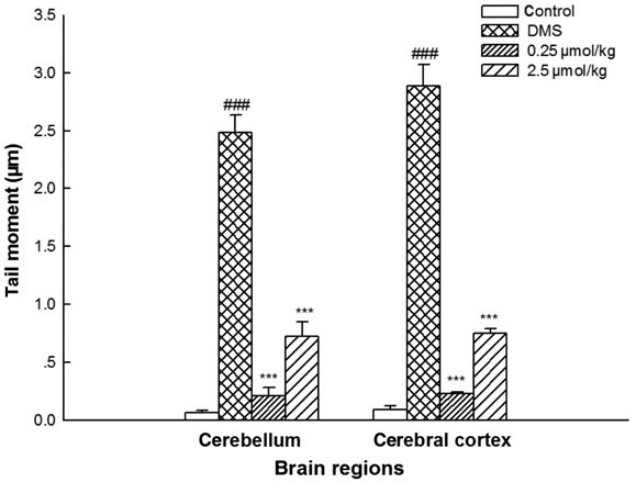

Figure 2. Effects of VAM on brain cells DNA-strand breaks in the cerebellum and cerebral cortex of mice. Two hundred cells were examined in duplicate for each condition and the tail moments are expressed as mean ± SEM, $^{***}P < 0.001$, VAM groups compared with control group. $^{###}P < 0.001$, DMS group compared with control group.

HPLC–ESI-MS^n analysis of VAM

VAM showed a protonated ion at m/z 410 at the retention time of 15.5 min in the LC–MS ion chromatogram (Figure 3A). As indicated in Figure 1, the MS^2 spectrum of VAM displayed ions at m/z 392, 375 and 295. The ion at m/z 392 was formed by the loss of a H_2O molecule, and could generate an ion at m/z 375 by further loss of an OH radical. The characteristic fragment ion at m/z 295 was formed as Part A by the loss of a piperidine ring moiety from the protonated VAM due to β-cleavage in the MS^2 spectrum. These fragment ions were used for structure elucidation of these metabolites with similar skeletons.

In vitro metabolic profiling

Analysis of the microsomal incubation samples of VAM with NADPH and the controls showed that four metabolic peaks (M1–M4) were generated in the *in vitro* samples (Figure 3B). In the MS^2 spectrum, M1 at 14.1 min showed a protonated molecule at m/z 426 and a main fragment ion at m/z 311, which were 16 Da higher than that of the protonated molecule of VAM at m/z 410 and its fragment ion at m/z 295 (Figure 4), indicating the formation of a hydroxyl group on Part A in the VAM structure. The MS^3 spectrum of M1 (426 → 311) showed the neutral losses of two H_2O moieties (Figure 5), suggesting the occurrence of hydroxylation at Site 1, 2, 3, 4, 7 or 11 rather than Site 20, due to steric effect. M2 at 14.6 min showed the same protonated molecule and characteristic fragment ions as M1 (Figure 4). The detected major fragment ion at m/z 311 resulted from hydroxylation at Part A by comparison with the corresponding ion at m/z 295 of VAM. The neutral loss of a H_2O moiety was observed in the MS^3 spectrum of M2 (426 → 311) (Figure 5), implying the occurrence of hydroxylation at site 15 or 16 to be 15-hydroxylveratramine or 16-hydroxylveratramine. M3 was eluted at 14.9 min with a protonated molecule at m/z 426.

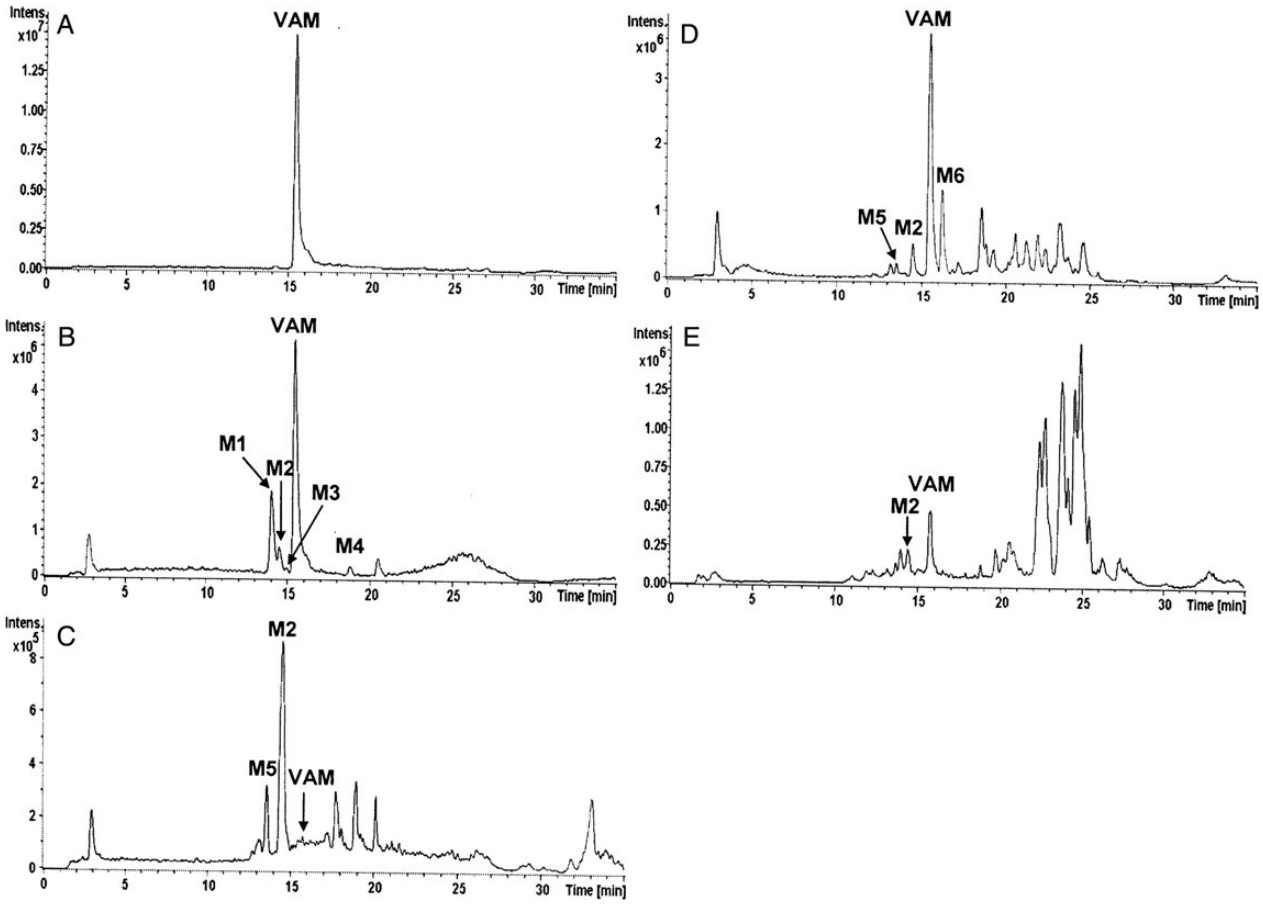

Figure 3. LC–MS ion chromatograms from metabolism studies of VAM: (A) VAM, (B) rat liver microsomal incubations with NADPH, (C) rat urine sample, (D) feces sample and (E) plasma sample.

The increase of 16 Da in molecular weight when compared with that of VAM and the characteristic fragment ion at m/z 295 was the same as that of VAM (Figure 4), indicating that Part A was intact. Moreover, neutral loss of 16 Da, which is typical for N-oxides (27), was not present in this case, confirming the occurrence of hydroxylation on the carbon atom of the piperidine ring moiety. M4 at 18.9 min had a longer retention time than that of VAM, and showed a protonated molecule at m/z 424, which was 14 Da higher than that of VAM. The characteristic fragment ion at m/z 295 was the same as that of VAM (Figure 4), suggesting that Part A was intact and the methylation occurred on the hydroxyl group at position 23 to be a methoxyl group in VAM.

Comparison of the ion chromatograms from the samples of VAM *in vitro* incubation with UDPGA and those from the controls showed that the peaks of protonated ion at m/z 586 were not found in the microsomal samples, while only one peak of protonated ion of VAM at m/z 410 was detected. The obtained results indicated that VAM did not undergo glucuronide conjugation, which was in agreement with the *in vivo* test (data not shown).

In vivo metabolic profiling

The extracted ion chromatograms of VAM at m/z 410 from the analysis of the pre- and postdose samples at different time points in the rat plasma, urine and feces showed the peak of VAM in the postdose samples while absent in the predose sample (Supplementary data, Figure S1), indicating no interference from the control samples on the detection of VAM. Since interference and ionization suppression induced by high-abundance endogenous metabolites could strongly prevent the detection of metabolites of VAM, we proposed a strategy for rapidly characterizing their structures in this study. First, the peaks corresponding to potential metabolites were determined from mass chromatogram comparisons between the pre- and postdose samples. Subsequently, the reasonable elemental composition difference could be determined based on the current understanding of potential biotransformation reactions (e.g., oxidation, sulfation, methylation, hydroxylation and glucuronidation). Finally, structural elucidation of these metabolites was performed by comparing their changes in molecular masses, retention times and spectral patterns with those of the parent drug.

VAM metabolites in rat urine

Two potential metabolites at m/z 426 (M2) and 442 (M5) existed in the postdose sample (Figure 3C), but not in the predose sample. Both of them had earlier retention times than VAM. Interestingly, there was no significant peak with a protonated ion at m/z 410 of the parent compound at the retention time

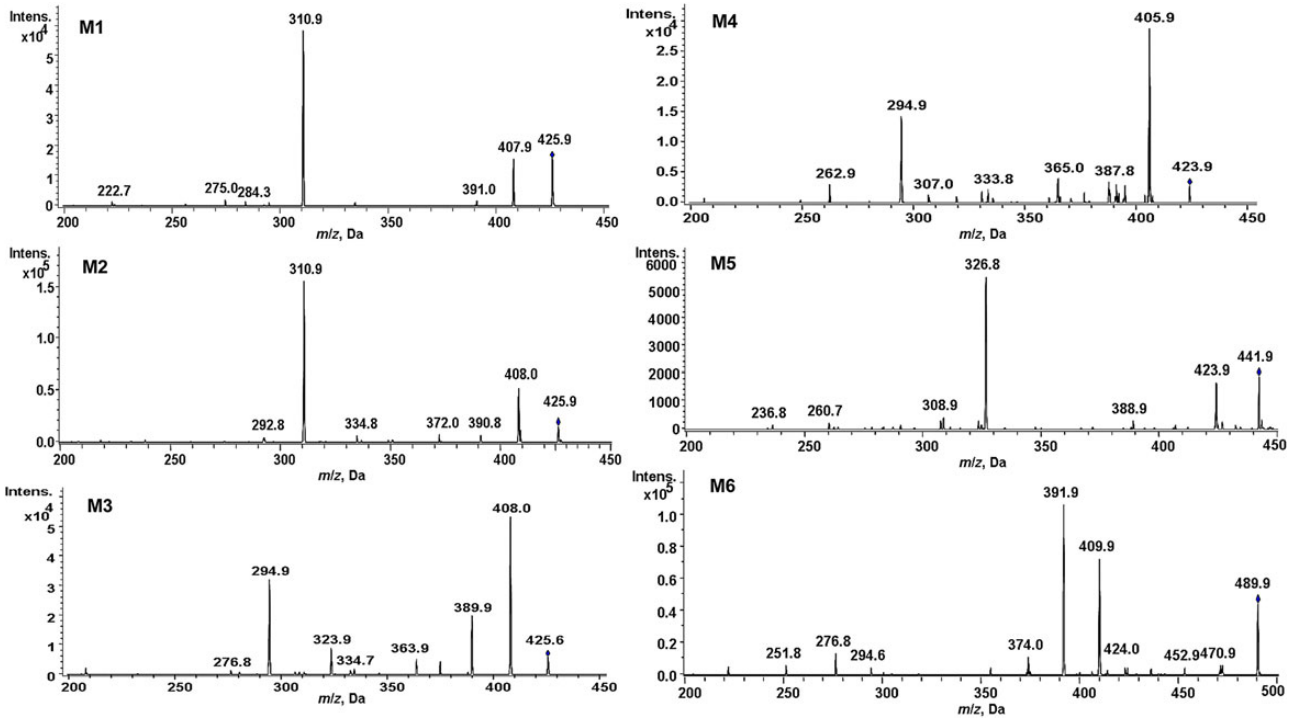

Figure 4. LC–MS-MS spectra from the analysis of M1–M6 of VAM.

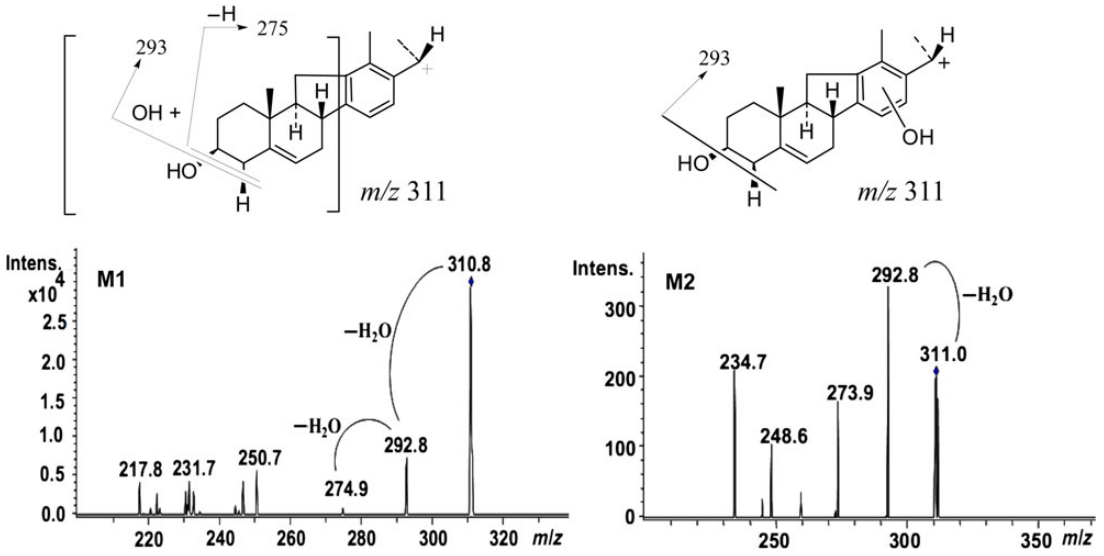

Figure 5. MS^3 spectra of m/z 426 → 311 for the analysis of M1 and M2.

of 15.5 min in the postdose urine sample. The metabolite with a protonated molecule at m/z 426 (M2) produced the same MS^2 spectrum, MS^3 spectrum and retention time as M2 identified in the *in vitro* samples. M5 at 13.5 min showed a protonated molecule at m/z 442 and a main fragment ion at m/z 327, which were 32 Da higher than that of VAM at m/z 410 and its fragment ion at m/z 295 (Figure 4), suggesting that modification occurred on Part A and M5 was generated by phenyl di-oxidation at sites 15 and 16 to form the metabolite of 15,16-dihydroxylveratramine (28).

VAM metabolites in rat feces

The three potential metabolites at m/z 426 (M2), 442 (M5) and 490 (M6) were observed in the postdose feces samples compared with predose samples (Figure 3D). The metabolites with protonated molecules at m/z 426 (M2) and 442 (M5) produced the same MS^2 spectra and retention time as M2 and M5 identified in rat urine. Unlike the urine sample, protonated VAM at retention time of 15.5 min was detected as the most abundant peak in the postdose sample, suggesting that VAM was mainly excreted in feces. M6 was eluted at 16.1 min and its molecular weight was

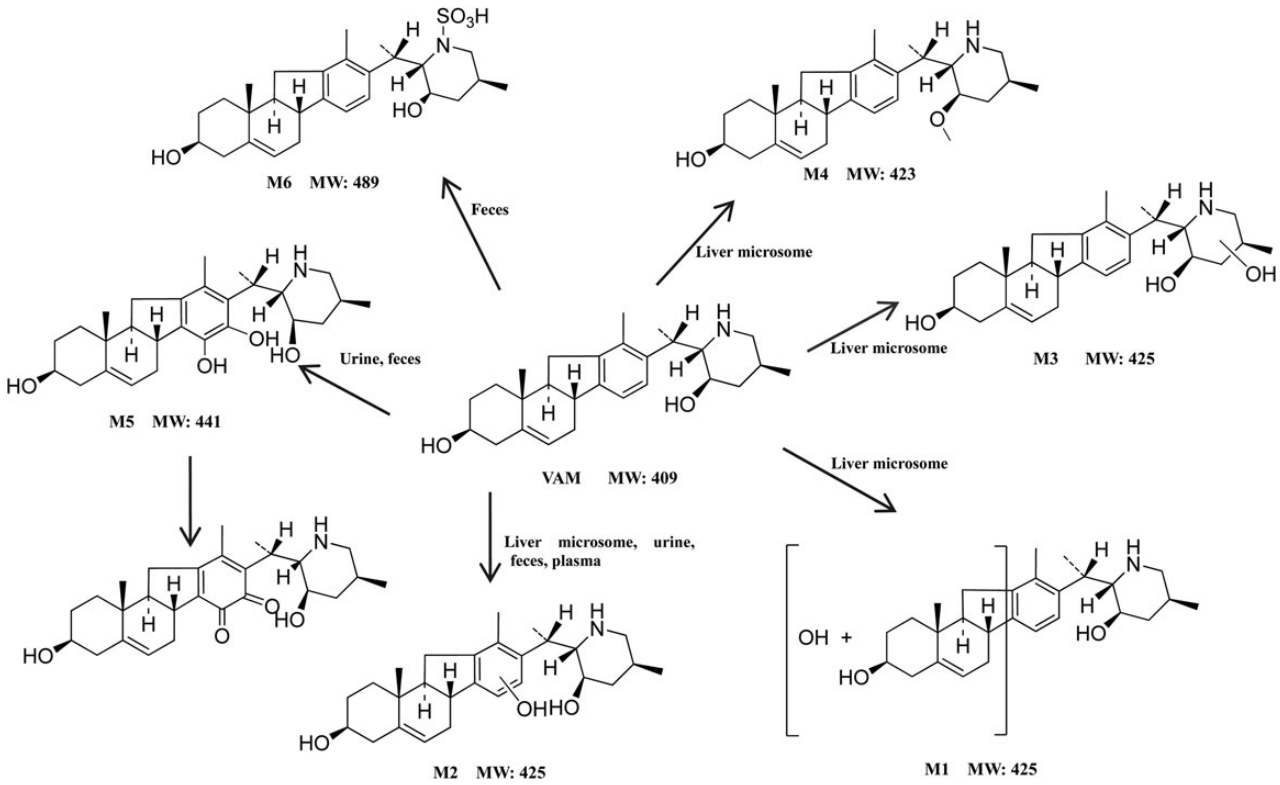

Figure 6. Proposed *in vivo* and *in vitro* metabolic pathways of VAM.

80 Da higher than that of VAM. The MS^2 spectrum of M6 showed the abundant fragment ion at m/z 410 formed by a loss of 80 Da, and the characteristic fragment ion at m/z 295 (Figure 4) was the same as that of VAM, confirming that Part A was intact and sulfate conjugation occurred on the nitrogen atom to be *N*-sulfoveratramine (28).

VAM metabolites in rat plasma

One more peak with a protonated ion at m/z 426 was observed in the postdose plasma samples compared with predose samples (Figure 3E). By performing MS^2 analysis and comparing the retention time, the compound corresponding to the peak at m/z 426 was identified as M2. It was noted that several intensive peaks existed at the end of plasma chromatogram. Analysis of extracted ions of potential VAM metabolites and tandem mass spectrometric spectra indicated that they were not related to the metabolism of VAM.

Discussion

To the best of our knowledge, this is the first investigation of *in vitro* and *in vivo* metabolites of VAM by using $LC-MS^n$. Based on the metabolite profile described above, the major metabolic pathways of VAM *in vivo* were proposed as phenyl mono-oxidation, sulfate conjugation and phenyl di-oxidation, whereas its *in vitro* metabolites were mainly produced from phenyl mono-oxidation, hydroxylation and methylation (Figure 6), suggesting that elimination of VAM occurred predominantly by oxidation. In the *in vitro* metabolism study, a protonated molecule ion at m/z 442 was detected, but the peak was very weak (data not shown). In addition, the trace amount of VAM in urinary excretion was the contribution of its lipophilicity. Thus, the fecal excretion of VAM in male rat played a dominant role in drug excretion. Sulfate conjugation for VAM as M6 might also be responsible for accelerate excretion of VAM *in vivo*.

The analysis of VAM metabolites showed that metabolic pathways were different between *in vitro* and *in vivo*, because the liver microsomal incubation could not reveal the *in vivo* physiological conditions. Lipophilic molecules may be attached to fractions of serum protein, e.g. albumin. Thus, the *in vitro* metabolism of substrates could differ significantly from the *in vivo* metabolism (29). On the other hand, some metabolites at trace concentrations may not be detected in animal bodies due to administration of low-dose VAM. Therefore, VAM methylation (M4) and monohydroxylation (M1 and M3) were only observed in the incubation with the rat liver microsomes.

The metabolites M2 and M5 were both from the phenyl oxidation of VAM, which could generate a catechol structure. The catechol structure may easily form highly electrophilic orthoquinone as toxic reactive metabolites catalyzed by mitochondrial dysfunction, inflammation, oxidative stress and dysfunction of the ubiquitin–proteasome system (30), which is responsible for neurotoxicity by formation of reactive oxygen species (ROS) to oxidize DNA and proteins (31, 32). Electrophilic quinones could also form covalent adducts with crucial cellular protein or DNA. Consequently, these quinone metabolites might be responsible for the VAM-induced DNA damages detected in mouse brain cells of cerebellum and cerebral cortex.

In summary, LC–MS^n was proved to be a powerful method to detect metabolites of VAM at trace levels. A full-scan MS followed by MS^2 analysis was adopted here to provide a more comprehensive *in vivo* and *in vitro* metabolic profile of VAM.

Conclusion

In this study, a HPLC–ESI-MS^n method was developed for the analysis of VAM and its *in vivo* and *in vitro* metabolites. Three metabolites were detected in rat feces samples, two were detected in urine and one was detected in plasma samples from the *in vivo* experiment, whereas four metabolites were detected in the *in vitro* samples with rat liver microsomes. Low- and high-dose VAM could both induce DNA damage in mouse brain cells of cerebellum and cerebral cortex. The oxidation of benzene ring in VAM would contribute to VAM-induced DNA damage by forming ROS and binding with biomacromolecule. The investigation on metabolic profiles of VAM might reveal *in vivo* biotransformation characteristic of *Veratrum* alkaloids, and provide crucial perspectives for their potential pharmaceutical applications and toxicity study.

Supplementary Material

Supplementary materials are available at *Journal of Chromatographic Science* (http://chromsci.oxfordjournals.org).

Funding

Financial support for this research was provided by grant from the Natural Science Foundation of China (no. 21102035).

References

1. Tang, J., Li, H.L., Huang, H.Q., Zhang, W.D.; Progress in the research on chemical constituents of Veratrum plants; *Progress in Pharmaceutical Sciences*, (2006); 30: 206–212.
2. Dobbs, M.R. (ed); Neurotoxic plants. In *Clinical neurotoxicology*, 1st ed., Chapter 2. E-Publishing, Inc., New York, NY, (2009), pp. 523–542.
3. Cong, Y., Zhang, Y.H., Guo, L., Wang, J.H.; *Veratrum japonicum* with genotoxicity on brain cells DNA of cerebellum and cerebral cortex in mice; *Chinese Traditional Patent Medicine*, (2011); 33: 1234–1236.
4. Freitasa, E.M.S., Fagianb, M.M., Höflinga, M.A.D.C.; Effects of veratrine and veratridine on oxygen consumption and electrical membrane potential of isolated rat skeletal muscle and liver mitochondria; *Toxicon*, (2006); 47: 780–787.
5. Crawford, L., Myhr, B.; A preliminary assessment of the toxic and mutagenic potential of steroidal alkaloids in transgenic mice; *Food and Chemical Toxicology*, (1995); 33: 191–194.
6. Cong, Y., Guo, L., Yang, J.Y., Li, L., Zhou, Y.B., Chen, J., *et al.*; Steroidal alkaloids from *Veratrum japonicum* with genotoxicity on brain cells DNA of cerebellum and cerebral cortex in mice; *Planta Medica*, (2007); 73: 1588–1591.
7. Keeler, R.F.; Teratogenic compounds of *Veratrum californicum* (Durand). *X. cyclopia* in rabbits produced by cyclopamine; *Neurotoxicology and Teratology*, (1970); 3: 175–180.
8. Niitsu, A., Harada, M., Yamagaki, T., Tachibana, K.; Conformations of 3-carboxylic esters essential for neurotoxicity in *Veratrum* alkaloids are loosely restricted and fluctuate; *Bioorganic and Medicinal Chemistry*, (2008); 16: 3025–3031.
9. Cong, Y., Zhou, Y.B., Chen, J., Zeng, Y.M., Wang, J.H.; Alkaloid profiling of crude and processed *Veratrum nigrum* L. through simultaneous determination of ten steroidal alkaloids by HPLC–ELSD; *Journal of Pharmaceutical and Biomedical Analysis*, (2008); 48: 573–578.
10. Wang, L.S., Li, W., Liu, Y.H.; Hypotensive effect and toxicology of total alkaloids and veratramine from roots and rhizomes of *Veratrum nigrum* L. in spontaneously hypertensive rats; *Die Pharmazie*, (2008); 63: 606–610.
11. Sanchez, P., Altaba, A.R.; *In vivo* inhibition of endogenous brain tumors through systemic interference of Hedgehog signaling in mice; *Mechanisms of Development*, (2005); 122: 223–230.
12. Tang, J., Li, H.L., Shen, Y.H., Jin, H.Z., Yan, S.K., Liu, X.H., *et al.*; Antitumor and antiplatelet activity of alkaloids from *Veratrum dahuricum*; *Phytotherapy Research*, (2010); 24: 821–826.
13. Thron, C.D., McCann, F.V.; Studies on the bradycardia and periodic rhythm caused by veratramine in the sinoatrial node of the guinea pig; *Journal of Electrocardiology*, (1998); 31: 257–268.
14. Keeler, R.J., Binns, W.; Teratogenic compounds of *Veratrum californicum* (Durand). 3. Malformations of the veratramine-induced type from ingestion of plant or roots; *Proceedings of the Society for Experimental Biology and Medicine*, (1967); 126: 452–454.
15. Nagata, R., Izumi, K., Iwata, S., Shimizu, T., Fukuda, T.; Mechanisms of veratramine-induced 5-HT syndrome in mice; *Japanese Journal of Pharmacology*, (1991); 55: 139–146.
16. Rajapakse, N., Butterworth, M., Kortenkamp, A.; Detection of DNA strand breaks and oxidized DNA bases at the single-cell level resulting from exposure to estradiol and hydroxylated metabolites; *Environmental and Molecular Mutagenesis*, (2005); 45: 397–404.
17. Sipinen, V., Laubenthal, J., Baumgartner, A., Cemeli, E., Linschooten, J.O., Godschalk, R.W.L., *et al.*; *In vitro* evaluation of baseline and induced DNA damage in human sperm exposed to benzo[a]pyrene or its metabolite benzo[a]pyrene-7, 8-diol-9, 10-epoxide, using the comet assay; *Mutagenesis*, (2010); 25: 417–425.
18. Lai, Y.Q., Cai, Z.W.; *In vitro* metabolism of hydroxylated polybrominated diphenyl ethers and their inhibitory effects on 17β-estradiol metabolism in rat liver microsomes; *Environmental Science and Pollution Research International*, (2012); 19: 3219–3227.
19. Ye, X., Wang, Y.G., Yang, M.H., Wang, Q.Q., Liang, Q.D., Ma, Z.C., *et al.*; Investigating the *in vitro* metabolism of veratridine: characterization of metabolites and involved cytochrome P450 isoforms; *Journal of Chromatography B*, (2009); 877: 141–148.
20. Cong, Y., Jia, W., Chen, J., Song, S., Wang, J.H., Yang, Y.H.; Steroidal alkaloids from the roots and rhizomes of *Vertrum nigrum* L.; *Helvetica Chimica Acta*, (2007); 90: 1038–1042.
21. Guo, L., Wang, L.H., Sun, B.S., Yang, J.Y., Zhao, Y.Q., Dong, Y.X., *et al.*; Direct *in vivo* evidence of protective effects of grape seed procyanidin fractions and other antioxidants against ethanol-induced oxidative DNA damage in mouse brain cells; *Journal of Agricultural and Food Chemistry*, (2007); 555: 881–5891.
22. Omura, T., Sato, R.; The carbon monoxide-binding pigment of liver microsomes I. evidence for its hemoprotein nature; *Journal of Biological Chemistry*, (1964); 239: 2370–2378.
23. Bradford, M.M.; A rapid and sensitive method for the quantitation of microgram quantities of protein utilizing the principle of protein-dye binding; *Analytical Biochemistry*, (1976); 72: 248–254.
24. Jin, X.Y., Han, G.Z., Huang, S.S.; Pharmacokinetics and cumulative toxicity of *Veratrum nigrum* L. var. ussuriense Nakai alkaloids in mice; *Pharmacology and Clinics of Chinese Materia Medica*, (2006); 22: 51–53.
25. Li, H.Y., Xu, W., Li, H.L., Zhang, W.D., Hu, L.W.; LC-MS-MS method for the determination of protoveratrine A in rat plasma; *Chromatographia*, (2009); 69: 523–529.
26. Kido, R., Sato, I., Tsuda, S.; Detection of *in vivo* DNA damage induce by ethanol in multiple organs of pregnant mice using the alkaline single cell gel electrophoresis (comet assay); *Journal of Veterinary Medical Science*, (2006); 68: 41–47.
27. Åberg, A.T., Löfgren, H., Bondesson, U., Hedeland, M.; Structural elucidation of *N*-oxidized clemastine metabolites by liquid chromatography/tandem mass spectrometry and the use of *Cunninghamella elegans* to facilitate drug metabolite identification; *Rapid Communications in Mass Spectrometry*, (2010); 24: 1447–1456.

28. Zeng, S. (ed). *Drug metabolism*. Zhejiang University Press, Hang Zhou, HZ, (2006), pp. 10–14.
29. Deglmann, C.J., Ebner, T., Ludwig, E., Happich, S., Schildberg, F.W., Koebe, H.G.; Protein binding capacity *in vitro* changes metabolism of substrates an influences the predictability of metabolic pathways *in vivo*; *Toxicology In Vitro*, (2004); 18: 835–840.
30. Rietjens, I.M.C.M., Awad, H.M., Boersma, M.G., van Iersel, M.L.P.S., Vervoort, J., Bladeren, P.J.V.; Structure activity relationships for the chemical behaviour and toxicity of electrophilic quinones/quinone methides; *Advances in Cirrhosis, Hyperammonemia, and Hepatic Encephalopathy*, (2001); 500: 11–21.
31. Miyazaki, I., Asanuma, M.; Approaches to prevent dopamine quinone-induced neurotoxicity; *Neurochemical Research*, (2009); 34: 698–706.
32. Bolton, J.L., Trush, M.A., Penning, T.M., Dryhurst, G., Monks, T.J.; Role of quinones in toxicology; *Chemical Research in Toxicology*, (2000); 13: 135–160.